

Measures of basins of attraction in spin-orbit dynamics

Alessandra Celletti · Luigi Chierchia

Received: 10 November 2007 / Revised: 4 March 2008 / Accepted: 1 April 2008 /
Published online: 23 May 2008
© Springer Science+Business Media B.V. 2008

Abstract We consider a dissipative spin-orbit model where it is assumed that the orbit of the satellite is Keplerian, the obliquity is zero, and the dissipative effects depend linearly on the relative angular velocity. The measure of the basins of attraction associated to periodic and quasi-periodic attractors is numerically investigated. The results depend on the interaction among the physically relevant parameters, namely, the orbital eccentricity, the equatorial oblateness and the dissipative constant. In particular, it appears that, for astronomically relevant parameter values, for low eccentricities (as in the Moon's case) about 96% of the initial data belong to the basin of attraction of the 1/1 spin-orbit resonance; for larger values of the eccentricities higher order spin-orbit resonances and quasi-periodic attractors become dominant providing a mechanism for explaining the observed state of Mercury into the 3/2 resonance.

Keywords Periodic attractors · Quasi-periodic attractors · Spin-orbit problem · Dissipative systems · Attraction bassins

1 Introduction and results

Nearly-integrable weakly-dissipative systems find many applications in Celestial Mechanics. As far as natural bodies are concerned several examples of nearly-integrable dissipative systems can be obtained considering the N -body gravitational problem with the influence of a dissipative force, like solar radiation, tidal torques, Yarkovsky effect, etc. As for artificial satellites, low-thrust spacecrafts provide an interesting example within Space Manifold Dynamics (i.e., a dynamical systems approach to spaceflight dynamics) of a nearly-integrable system with a small dissipation due to the slow loss of mass during the travel.

A. Celletti (✉)
Dipartimento di Matematica, Università di Roma Tor Vergata, 00133 Roma, Italy
e-mail: celletti@mat.uniroma2.it

L. Chierchia
Dipartimento di Matematica, Università "Roma Tre", 00146 Roma, Italy
e-mail: luigi@mat.uniroma3.it

In order to investigate analytically such systems, the starting point is the derivation of a proper mathematical model apt to explain the astronomical behavior. Different studies in this direction have been worked out during the past decades, both in the conservative and dissipative setting. Typically, the study in the conservative framework was based on the existence of invariant tori, while in the dissipative case much effort was devoted to compute a probability of capture into resonance.

As a concrete example, we consider the spin-orbit interaction with tidal dissipation. More precisely we study the motion of a triaxial satellite rotating around a primary body under the following simplifying assumptions: the trajectory of the center of mass of the satellite is assumed to be a Keplerian orbit, the obliquity is set to zero, the rotation axis is assumed to coincide with the smallest physical axis. Within the dissipative effects the strongest contribution is provided by the tidal friction due to the internal non-rigidity of the satellite. As in [Correia and Laskar \(2004\)](#), we consider a dissipative force with a phase lag depending linearly on the relative angular velocity (see also [Goldreich and Peale \(1966, 1970\)](#); [MacDonald \(1964\)](#); [Peale \(2005\)](#)). The equation of motion governing such model is described by a second-order time-dependent differential equation. Three physical parameters enter into the model: the orbital eccentricity, the equatorial oblateness and the dissipative constant. The values of these parameters rule the dynamics and in particular affect the existence of periodic orbit attractors, which are related to spin-orbit resonances occurring whenever the periods of revolution and of rotation are commensurate.

Generally speaking, the dynamics of dissipative nearly-integrable systems reveals a very rich structure composed by periodic orbits, invariant tori and (periodic/quasi-periodic/strange) attractors. In the purely conservative regime, periodic orbits exist for all rational periods and many quasi-periodic tori exist thanks to KAM theory,¹ while, when the dissipation is turned on, at most one quasi-periodic attractor may exist, provided the “driving frequency” is suitably related to the angular velocities; ([Celletti and Chierchia 2008](#)) and co-existence with many periodic orbits (spin-orbit resonances) is possible ([Broer et al. 1996, 1998](#)).

Astronomical observations show that a large number of satellites of the solar system moves in (or close to) a synchronous periodic orbit (i.e., a 1/1 resonance), always pointing the same face to the host planet. Only Mercury is observed in a 3/2 spin-orbit resonance, namely it completes three rotations about its spin axis during two orbital revolutions around the Sun. An example of chaotic rotation has been provided by Hyperion, since its spin axis is tumbling chaotically in space ([Wisdom et al. 1984](#)). At the light of the phenomenology presented by celestial bodies, the basic question concerning the spin-orbit interaction is: *Why nature seems to have selected only the 1/1 and 3/2 resonances?*

This work tries to contribute to the understanding of the spin-orbit resonances, by proposing an explanation of the actual state of the rotational dynamics based on the existence of periodic and quasi-periodic attractors associated to the dissipative spin-orbit problem. In the weakly dissipative regime, periodic attractors may be easily analytically shown to coexist ([Biasco and Chierchia 2008](#)). The quasi-periodic case is more difficult in view of the appearance of small divisors and it was proved in [Celletti and Chierchia \(2008\)](#) that KAM tori smoothly bifurcate into quasi-periodic attractors for the dissipative system, provided that the “driving frequency” is suitably tuned with the parameters of the model.

Here, for physical values of the parameters, we investigate numerically the occurrence of periodic and quasi-periodic attractors by computing the *basin-of-attraction measure* (hereafter *BAM*) as follows. For each parameter sample, we consider 1000 initial conditions by a

¹ See [Arnold \(1988\)](#) and [Celletti and Chierchia \(2006\)](#), for generalities, and [Celletti \(1990\)](#) for the spin-orbit case.

Monte–Carlo method; then we integrate the equation of motion using Yoshida’s algorithm up to a long, experimentally determined, transient time. Once the leading attractors are detected, we compute their frequency and we define the corresponding BAM by counting the percentage of the initial data which have evolved toward the attractor. As in [Colombo and Shapiro \(1966\)](#), [Goldreich and Peale \(1966, 1970\)](#) or [Henrard \(1985\)](#), also the analysis presented here clearly indicates that the dynamics is strongly affected by the orbital eccentricity: dissipative forces contribute to drive the body toward the attractor whose frequency depends on the value of the eccentricity of the Keplerian orbit around which the satellite is orbiting.

For the Moon’s parameter values ($e = 0.0549$), the 1/1 resonance is characterized by a high BAM (over 95%) for all values of the dissipative constant considered. In the case of Mercury ($e = 0.2056$) the results show that an invariant attractor with asymptotic frequency of 1.256 is likely to attract about 73% of the initial data, while the 3/2 resonance has a BAM of 14% vs. 5% associated to the 5/4 resonance and 6% to the synchronous resonance (the rest pertains to the 2/1, 5/2 and 3/1 commensurabilities).

We stress that the BAM as defined in this paper is merely a measure of the basins of attraction of a given (quasi-)periodic attractor and does not take into account any geometrical information. For example, at contrast with other semi-analytical methods, such as the Goldreich and Peale approach (see below), the BAM does not say anything regarding *how* the limiting regime is achieved, nor where, in phase space, the dynamics evolution takes place.

In [Correia and Laskar \(2004\)](#) it has been shown that the eccentricity of Mercury might have undergone, over large time scales, strong variations reaching the value of the eccentricity $e \simeq 0.3$; our results indicate that for $e \simeq 0.28$ the 3/2 BAM has a peak above 90%, while for lower values of the eccentricity quasi-periodic attractors show up with relatively high BAM. Since quasi-periodic attractors separate the phase space, their appearance—in an evolutionary model which takes into account variations over relative long time scales of the orbital parameters—may be interpreted as a trapping mechanism preventing the evolution of Mercury into the 1/1 spin-orbit resonance.

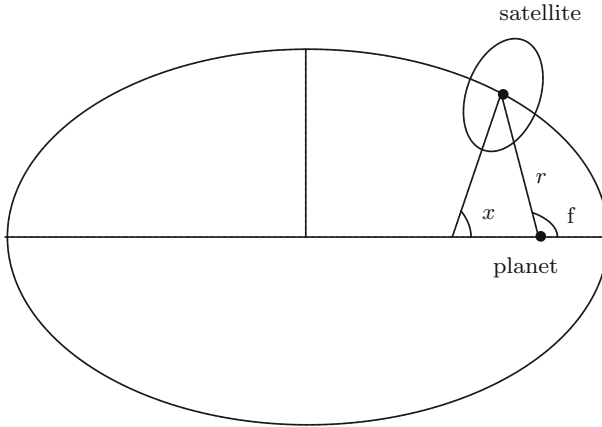
Finally, we compare the values of the BAM, as computed in this paper, with the values obtained by the Goldreich and Peale probability-of-capture formula, which, as well known, is an analytic approximate expression obtained (after a suitable averaging procedure) in order to compute the probability of evolving towards and remaining captured by a given spin-orbit resonance (see [Goldreich and Peale \(1966, 1970\)](#) and, for an interpretation in terms of adiabatic invariant theory, ([Henrard 1985](#))). In doing such comparison one should, however, keep in mind the relevant differences, both theoretical and computational, between the two methods. Notice, in particular, that our method does not say anything about what happens at the *boundary* of the basins of attraction, which is a clearly interesting problem and which might be related with the Goldreich and Peale probability-of-capture formula (compare, in particular to [Henrard 1985](#)).

2 The model

We consider a triaxial satellite S which rotates around an internal spin-axis and orbits about a central planet. We investigate a simplified model where the mass center of the satellite is assumed to move on a given Keplerian orbit of eccentricity e around the planet (or the Sun, in the Mercury case); the rotation axis is taken to be constantly perpendicular to the orbital plane and coinciding with the smallest physical axis of the satellite. Moreover, we assume that a dissipative tidal torque $T = T(\dot{x}; t)$ acts on the system. We normalize to unity the mean motion $n = \frac{2\pi}{P_{\text{rev}}}$, where P_{rev} is the orbital period of the satellite; the equation of motion can be written as follows (see [Peale \(2005\)](#)):

$$\ddot{x} + \varepsilon \left(\frac{a}{r}\right)^3 \sin(2x - 2f) = T(\dot{x}; t), \tag{1}$$

where, ε denotes the equatorial oblateness of the satellite and it is given by $\varepsilon \equiv \frac{3}{2} \frac{B-A}{C}$, $A < B < C$ being the principal moments of inertia; a is the semimajor axis of the Keplerian orbit; $r = r(t)$ is the instantaneous orbital radius; $f = f(t)$ is the true anomaly; x is the angle, in the orbital plane, formed by the direction of the longest axis of the ellipsoid and the perihelion line (see figure below).



Since the center of mass of the satellite is assumed to revolve on an assigned Keplerian orbit, the quantities r and f are known 2π -periodic functions of time t (recall that the mean motion has been normalized to one), which are implicitly determined via the Keplerian relations:

$$\begin{cases} t - t_0 = u - e \sin u \\ r = a(1 - e \cos u) \\ f = 2 \arctan \left(\sqrt{\frac{1+e}{1-e}} \tan \frac{u}{2} \right) \end{cases} \tag{2}$$

(t_0 is an “initial reference” time of observation, which we shall take to be zero).

Let us remark that if the tidal torque vanishes, (1) becomes the evolution equation of a Hamiltonian (conservative) system, which, in turn, becomes integrable whenever either $e = 0$ (the Keplerian orbit is a circle) or $\varepsilon = 0$ (the satellite has a circular equator).

Considering the lift of the angle x on \mathbf{R} , we define a *spin-orbit resonance of type p/q* (and order $p + q$), for two relatively prime integers p, q with $q > 0$, as a solution of (1) $t \in \mathbf{R} \rightarrow x = x(t) \in \mathbf{R}$ such that

$$x(t + 2\pi q) = x(t) + 2\pi p, \quad \forall t \in \mathbf{R} .$$

This relation means that during q revolutions around the planet, the satellite makes p rotations about its spin-axis. As is well known the Moon (as well as many other satellites of the solar system) is observed to move in a 1/1 resonance; a remarkable exception is provided by Mercury which is observed in a 3/2 spin-orbit resonance.

We next specify the analytical form of the tidal torque T . Assuming a phase lag depending linearly on the relative angular velocity (Correia and Laskar 2004; Goldreich and Peale 1966; MacDonald 1964; Peale 2005) and denoting by K a dissipative constant depending on the

physical and orbital features of the satellite, we assume that the dissipative torque takes the form (Peale 2005)

$$T(\dot{x}; t) = -K [L(e, t)\dot{x} - N(e, t)], \tag{3}$$

with

$$L(e, t) = \frac{a^6}{r^6}, \quad N(e, t) = \frac{a^6}{r^6}\dot{t}.$$

A further simplification may be obtained by assuming (as in Correia and Laskar 2004) that the dynamics is essentially ruled by the average of $L(e, t)$ and $N(e, t)$ over one orbital period:

$$\bar{T} := \bar{T}(\dot{x}) = -K [\bar{L}(e)\dot{x} - \bar{N}(e)] \tag{4}$$

with (see Peale (2005))

$$\begin{aligned} \bar{L}(e) &:= \frac{1}{(1 - e^2)^{9/2}} \left(1 + 3e^2 + \frac{3}{8}e^4 \right) \\ \bar{N}(e) &:= \frac{1}{(1 - e^2)^6} \left(1 + \frac{15}{2}e^2 + \frac{45}{8}e^4 + \frac{5}{16}e^6 \right). \end{aligned} \tag{5}$$

In Appendix, we point out that numerical comparisons between the model defined through the time dependent functions $L(e, t)$ and $N(e, t)$ (see (3)) with the model where these functions are replaced by their averages over a period (see (4)) are in remarkable agreement.

We are finally led to consider the following equation of motion (compare with Correia and Laskar 2004):

$$\ddot{x} + \varepsilon \left(\frac{a}{r}\right)^3 \sin(2x - 2f) = -\eta(e)[\dot{x} - \nu(e)], \tag{6}$$

with $f = f_e(t)$ and $r = r_e(t)$ implicitly defined in (2), and with

$$\eta(e) := K\bar{L}(e), \quad \nu(e) := \frac{\bar{N}(e)}{\bar{L}(e)} = \frac{1}{(1 - e^2)^{3/2}} \frac{1 + \frac{15}{2}e^2 + \frac{45}{8}e^4 + \frac{5}{16}e^6}{1 + 3e^2 + \frac{3}{8}e^4}. \tag{7}$$

The function $\eta(e)$ measures the strength of the dissipation while the function $\nu(e)$ (which is a monotone increasing function of e and takes values between 1 and $+\infty$) plays the role of a “driving frequency”.

Notice that when $\varepsilon = 0$ but $K \neq 0$, (6) admits a *global attractor*: in fact, the general solution of (6) when $\varepsilon = 0$ and $K \neq 0$ is given by

$$x(t) = x(0) + \nu t + \frac{1 - e^{-\eta t}}{\eta} (\nu(0) - \nu),$$

where $(x(0), \nu(0))$ denote, respectively, the initial position and velocity; thus the particular solution $x(t) = x(0) + \nu t, \dot{x}(t) = \nu$ is a global attractor; we point out that such attractor is *quasi-periodic* for any ν irrational (remember that $(x, t) \in \mathbf{T}^2$).

We next remark that the astronomical observations suggest that for the Moon and Mercury the value of ε is of the order of 10^{-4} , while the order of magnitude of K (and, hence, of η) is about 10^{-8} (Correia and Laskar 2004; Cox 2000; Peale 2005).

In the parameter region of interest for us, i.e., $|\eta| < \varepsilon \ll 1$, periodic attractors for (6), together with their positive measure of basins of attraction, may be analytically shown to coexist for the main low-order resonances (see Biasco and Chierchia 2008). On the other hand, quasi-periodic solutions, i.e. solutions of the form $x(t) = \omega t + u(\omega t, t)$ with ω irrational and

$u(\theta_1, \theta_2)$ 2π -periodic in each variables θ_i , do not always exist: they exist only for Diophantine frequencies ω and provided the driving frequency ν is sharply tuned with ω so that, in particular, $\nu = \omega + O(\varepsilon^2)$ (see [Celletti and Chierchia 2008](#)); however, when such quasi-periodic attractors exist, they are unique and seem to have a large BAM, as shown below.

3 Measuring basins of attraction

As is well known (see, e.g., [Feudel et al. 1996](#) or [Biasco and Chierchia 2008](#) for the spin-orbit case) for specific values of the parameters, periodic orbit attractors may coexist. For $\varepsilon = 0$ the frequency ω of the attractor is linked to the eccentricity e by the relation $\omega = \nu(e)$ with $\nu(e)$ defined in (7). We analyze quasi-periodic attractors as well as low-order resonances of the form $\frac{p}{q}$ with $p, q \leq 5$ and $\frac{p}{q} \leq 3$; moreover, we focus on the eccentricities of the Moon ($e = 0.0549$) and Mercury ($e = 0.2056$) corresponding, respectively, to driving frequencies $\nu = 1.01809$ and $\nu = 1.25584$.

In order to obtain reliable numerical data, we integrate the equation of motion (using Yoshida's algorithm ([Yoshida 1990](#)) letting the dynamics evolve for a long, experimentally determined, *transient time* $T_K \simeq 10^3/K$. Such transient time gives a strong limitation on the computer time needed in our experiments and for $K = 10^{-8}$ (which is, presumably, the correct value for the Moon and Mercury), T_K goes far beyond our computer capabilities, and, therefore, we had to limit our investigations to values of the dissipative parameter ranging between 10^{-3} and 10^{-6} (values which have, nonetheless, physical relevance for some satellites of the solar system).

For each parameter sample, we measure the basins of attraction by counting the number of initial data which evolve, after time T_K , on a specific attractor. More precisely, by a Monte-Carlo method we consider 1,000 initial conditions $(x(0), \dot{x}(0))$ in the compact region $\{0 \leq x \leq 2\pi, 0 \leq \dot{x} \leq 5\}$; we integrate the equations of motion and let the dynamics evolve up to the transient time T_K and detect the leading attractors; finally, we compute the frequencies ω of the detected attractors and calculate the relative BAM by counting the percentage of the initial data which have approached them.

We underline that the BAM as defined here is a "global indicator" and does not reflect the geometry of the boundary of the basins of attractions, nor gives any information about the motions in a neighborhood of such boundaries.

We also observe that, in general, for a given eccentricity e_0 the highest occurrences correspond to the attractors with $\omega \simeq \nu(e_0)$ (as already noticed, e.g., in [Goldreich and Peale \(1966, 1970\)](#)).

In [Table 1](#) we report the results obtained taking $\varepsilon = K = 10^{-4}$ for $e = 0.0549$ (Moon's case) and $e = 0.2056$ (Mercury's case). For the Moon's eccentricity there appear only the 1/1 periodic attractor and the invariant curve with frequency $\nu(0.0549) \simeq 1.018$. On the other hand, for $e = 0.2056$ the 1/1 and the 3/2 resonances have approximately the same (low) BAM, while the invariant attractor with frequency $\nu(0.2056) \simeq 1.256$ plays a dominant role.

Next we try to better understand the effect of the dissipative constant; having fixed $\varepsilon = 10^{-3}$ we report in [Tables 2](#) and [3](#) the different attractors and the corresponding percentages of initial data evolving towards them. For the Moon ([Table 2](#)), there appear only periodic orbit attractors corresponding to the 1/1, 3/2 and 2/1 resonances. In the case of Mercury ([Table 3](#)) there exist different periodic attractors (with frequencies 1, 5/4, 3/2, 2, 5/2, 3) and an invariant curve attractor with rotation number $\omega \simeq \nu(0.2056) \simeq 1.256$. In both cases the value of K has been decreased from $K = 10^{-3}$ down to $K = 5 \cdot 10^{-6}$, while the result for $K = 10^{-6}$ appearing in [Tables 2](#) and [3](#) (denoted in italics and marked with an asterisk)

Table 1 Basin of attraction measure for $\varepsilon = 10^{-4}$ and $K = 10^{-4}$

<i>Moon</i> ($e = 0.0549$)	$\omega = 1/1$ 9.3%	$\omega = 1.018$ 90.7%	
<i>Mercury</i> ($e = 0.2056$)	$\omega = 1/1$ 1%	$\omega = 1.256$ 97.5%	$\omega = 3/2$ 1.5%

For each frequency ω of the attractor we provide the percentage of initial data which are attracted

Table 2 BAM for $e = 0.0549$ (“Moon case”), $\varepsilon = 10^{-3}$ and different values of K ; last value is obtained by interpolating the previous data through a degree 8 polynomial

K	$\omega = 1/1$	$\omega = 3/2$	$\omega = 2/1$
10^{-3}	100%	–	–
$5 \cdot 10^{-4}$	100%	–	–
10^{-4}	98.3%	1.7%	–
$5 \cdot 10^{-5}$	97.4%	2.6%	–
10^{-5}	97.6%	2.1%	0.3%
$5 \cdot 10^{-6}$	96.7%	3%	0.3%
$10^{-6}(*)$	95.8%	3.9%	0.3%

For each frequency ω of the attractor, we provide the percentage of initial data which are attracted by the attractor over a sample of 1000 randomly chosen points

Table 3 “Mercury case”: as in Table 2 but for $e = 0.2056$, $\varepsilon = 10^{-3}$

K	1/1	5/4	1.256	3/2	2/1	5/2	3/1
10^{-3}	2%	–	92.3%	5.7%	–	–	–
$5 \cdot 10^{-4}$	3.9%	1%	87.5%	7.6%	–	–	–
10^{-4}	4.4%	6%	76.9%	10.9%	1.8%	–	–
$5 \cdot 10^{-5}$	4.4%	7.7%	72.7%	11.6%	3%	0.6%	–
10^{-5}	4.7%	8.4%	69.8%	12.6%	2.9%	1.1%	0.5%
$5 \cdot 10^{-6}$	4.7%	6.8%	71.6%	13.3%	2.7%	0.6%	0.3%
$10^{-6}(*)$	4.6%	5.1%	73.4%	14%	2.5%	0.2%	0.2%

has been computed by interpolating (with a degree 8 polynomial) the data corresponding to the previous values of K .

By analyzing the results of Table 2 we notice that for the Moon the 1/1 resonance dominates for all values of K ; decreasing the dissipative constant there start to appear different resonances and precisely the 3/2 and the 2/1, though their BAM is definitely lower compared to that of the synchronous resonance.

A different situation occurs for Mercury (Table 3), where many different resonances emerge as K decreases. Looking at Table 3 the direct perception is that the invariant curve attractor with $\omega \simeq \nu(0.2056) \simeq 1.256$ dominates, though the 3/2 and 5/4 resonances are marked by a relatively high BAM with respect to the other resonances.

Next, we analyze the behavior of the BAM with respect to a variation of the eccentricity. More precisely, we consider fixed values of the perturbing and dissipative parameters, say $\varepsilon = 10^{-3}$ and $K = 10^{-4}$ as in Fig. 1, while the orbital eccentricity is varied within a sample of 100 values between 0 and 0.5 with step-size 0.005. Figure 1 shows the main resonances (1/1, 3/2, 2/1, 5/2); for a given eccentricity the points corresponding to the label ‘invariant’ correspond to the quasi-periodic attractors whose frequency can be approximately computed

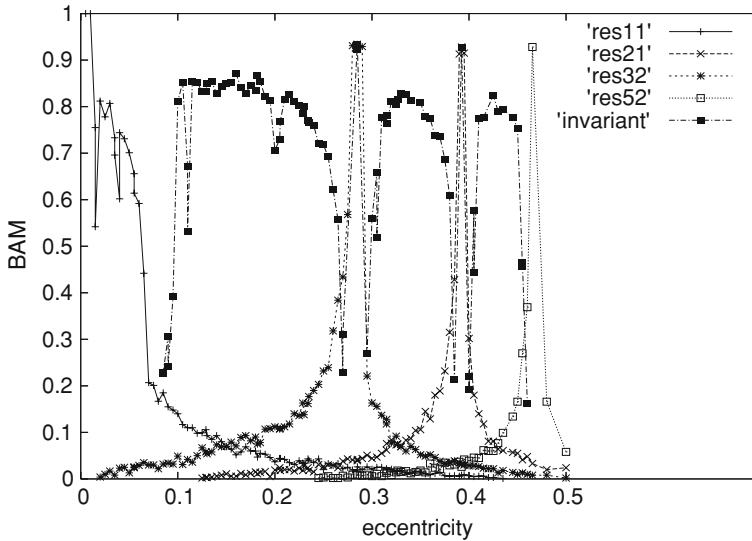


Fig. 1 Measure of the basin of attraction (BAM) for a sample of 100 eccentricities with step-size 0.005; the parameters are $\varepsilon = 10^{-3}$ and $K = 10^{-4}$. Each curve corresponds to a different frequency; for example, 'res11' is associated to the frequency $\omega = 1$, 'res52' to $\omega = 5/2$ and so on. The label 'invariant' is associated to the invariant attractor with frequency $\omega \simeq \nu(e)$ as computed in (7). The behavior of the resonances 1/1, 2/1, 3/2, 5/2 and of the invariant attractors is displayed

through (7). For low eccentricities the 1/1 resonance dominates, while the 3/2 resonance dominates around $e = 0.28$; the 2/1 resonance has a peak around $e = 0.39$ and the 5/2 resonance attains its maximum for very large eccentricities. Between the peaks corresponding to the spin-orbit resonances there appear large parameter regions where the invariant attractors dominate.

A different situation occurs as the parameters are varied, as, for example, in the case of Fig. 2 where $\varepsilon = 10^{-1.5}$ and $K = 10^{-3}$ (i.e., $K = \varepsilon^2$). The resonant attractors show a behavior similar to that presented in Fig. 1, while the invariant attractor almost disappears.

Finally, we compare, for some chosen parameter values, the BAM, as numerically evaluated in this paper, with the well known *probability capture* P_{capt} , as derived by Goldreich and Peale (1966, 1970) and later reinterpreted, in terms of adiabatic invariant theory, by Henrard (1985). The results are reported in Table 4.

As one can see, there is a relatively good agreement as far as the 3/2 resonance is concerned, but there are also a few discrepancies, as, for example, for the 1/1. Clearly, in making this comparison, one has to keep in mind that the Goldreich–Peale capture probability is evaluated in terms of a formula derived after several approximations,² while our approach is based upon direct (numerical) integration of the full model; furthermore, as already mentioned, the BAM is a global indicator and does not distinguish what happens in a neighborhood of the boundary of basins of attraction, while the Goldreich and Peale analysis (see, also, the Hamiltonian discussion in Henrard 1985) is suited to give information about the evolution of data close to instability regions so as to determine the eventual “capture” by a particular resonance.

² The Goldreich–Peale formula is based upon an averaging of the Newtonian potential and, in particular, does not depend explicitly upon the dissipative parameter K , which plays a major role in our analysis.

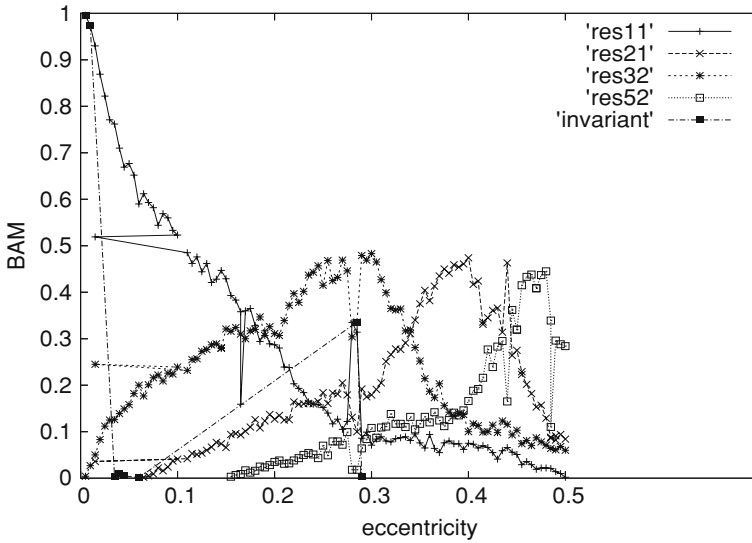


Fig. 2 As in Fig. 1, but with parameters $\epsilon = 10^{-1.5}$ and $K = \epsilon^2 = 10^{-3}$

Table 4 Comparison between the probability capture P_{capt} calculated according to the Goldreich and Peale formula and the extrapolated BAM for the “Mercury case” ($e = 0.2056$, $\epsilon = 10^{-3}$, $K = 10^{-6}$); compare Table 3

	1/1	5/4	1.256	3/2	2/1	5/2	3/1
P_{capt}	0%	–	–	17.4%	4.3%	1.8%	–
BAM	4.6%	5.1%	73.4%	14%	2.5%	0.2%	0.2%

4 Conclusions

In the *conservative* spin-orbit problem for suitable values of the parameters one can find a multitude of invariant tori with irrational winding number and periodic orbits of any period; furthermore, periodic orbits can be used to approximate KAM tori by taking sequences of periodic orbits with frequency given by the rational approximants of the winding number.

In the *dissipative* spin-orbit problem the situation is drastically different, since one can find at most one (smooth) quasi-periodic invariant attractor, though the dynamics can be also attracted toward a number of coexisting periodic orbits. However, for typical astronomical values of the parameters, only low-order resonances (1/1, 5/4, 3/2, 2/1, 5/2 and 3/1) seem to dominate, a fact that is partially confirmed by the theory in [Biasco and Chierchia \(2008\)](#).

Keeping this in mind we have studied periodic and quasi-periodic attractors by looking at their behavior as the main parameters are varied, namely, the eccentricity, the equatorial oblateness and the dissipative constant. We have provided a measure for the basins of attraction simply by computing the percentage of initial conditions evolving to the attractor; not surprisingly, the results show that the occurrence of attractors strongly depends on the value of the eccentricity through the relation (7).

A first conclusion is that the synchronous resonance heavily dominates when the eccentricity is small (like for the Moon), while higher order resonances appear as the eccentricity increases.

Furthermore, a number of conclusions can be drawn by looking at the data corresponding to Mercury's eccentricity. First, there happen to exist an invariant attractor with frequency between the 1/1 and 3/2 resonances, actually lying very close to the 5/4 resonance since its rotation number amounts to about 1.256. This attractor is characterized by a large BAM and its existence prevents the dynamics "above" the attractor to move toward the 1/1 resonance (see below). Moreover, within the resonances which arise for low values of K , the 3/2 resonance most likely captures the majority of initial data.

However, let us remark that these results do not exploit the evolutionary history of the planet, as done in [Correia and Laskar \(2004\)](#), where the perturbations induced by the other bodies of the solar system on Mercury's eccentricity are taken into account. More precisely, according to [Laskar \(1996\)](#), Mercury's eccentricity experienced large excursions from $e \simeq 0.1$ to $e \simeq 0.3$. The upper value is compatible with the capture of Mercury in a 3/2 resonance, corresponding to an eccentricity about equal to 0.285 (namely $\nu(0.285) \simeq 1.5$); our results (see Fig. 1) show that for such value the BAM is around 93%, while for lower eccentricities there exist quasi-periodic attractors with higher BAM. The existence of quasi-periodic attractors provides a strong confinement property (at least, according to the low-dimension model considered here), due to the fact that they separate the phase space; therefore, as the eccentricities vary according to an evolutionary model a trapping mechanism might have prevented Mercury to evolve toward the synchronous resonance. Furthermore, we have shown that the decrease of the dissipative effects contributes to increase the BAM of the 3/2 resonance. We remark that this scenario does not hold for the Moon, since its eccentricity is too low to lead to a capture in a non-synchronous resonance.

The results presented in this paper indicate that the present spin-orbit resonant state of the celestial bodies might be explained by using a nearly-integrable dissipative model. Indeed, the entangled structure of the phase space in the conservative framework is thinned out by the dissipation, whose action contributes to leave at most one quasi-periodic attractor and a few periodic orbits. Based on this scenario, in agreement with [Colombo and Shapiro \(1966\)](#) we have provided a possible explanation of the present state of Mercury in a 3/2 resonance by means of the interaction of two factors: the high orbital eccentricity and the effect of the dissipative tidal torque.

The analysis of the results provided in this work opens many questions in the framework of the dissipative spin-orbit problem or, more generally, of weakly-dissipative nearly-integrable systems. To outline future lines of research, we mention, for example: the investigation of the relation between periodic and quasi-periodic attractors: in particular, the analysis of the behavior at the boundary of the basins of attractions and relations with the Goldreich–Peale probability of capture; the generalization of the results to a model with non-zero obliquity and, more in general, to more realistic models; the evolution of Mather sets in the dissipative setting; the dependence of the results upon the form of the dissipation.

Appendix: Time-dependent dissipation

In order to discuss the validity of the model (6) we compare the tidal-averaged model with that including the time-dependent tidal force. More precisely, with reference to (3) we expand r and \dot{f} in powers of the eccentricity; neglecting terms of order 5 one obtains ([Peale 2005](#))

$$T(\dot{x}; t) = -K [L_5(e, t)\dot{x} - N_5(e, t)] \quad (\text{A.8})$$

with

Table A.1 Computation of the BAM for different eccentricities with $\varepsilon = 10^{-3}$ and $K = 10^{-4}$

e	$\omega = 1$	$\omega = 3/2$	$\omega = 2$	'invariant'
0.0549	98.4%; 98.3%	1.6%; 1.7%		
0.08	14.2%; 13.6%	2.6%; 3.9%		83.2%; 82.5%
0.1	15.7%; 12.2%	4.6%; 4.8%		79.7%; 83%
0.12897	8.3%; 9.1%	6.8%; 6.9%	0.1%; 0.1%	84.8%; 83.9%

The rows indicate different eccentricities, while the columns denote the frequencies of the attractors (the column 'invariant' corresponds to the frequency of the invariant attractor associated to the given eccentricity through (7)). Two models of tidal friction are considered: the time-dependent formulation (A.8)–(A.9) and the averaged model (4)–(5); the first number corresponds to the percentage obtained through the time-dependent model, while the second number is the percentage derived from the averaged model

$$\begin{aligned}
 L_5(e, t) &= 1 + \frac{15}{2}e^2 + \frac{105}{4}e^4 + 6e \cos t + \frac{117}{4}e^3 \cos t + \frac{27}{2}e^2 \cos(2t) \\
 &\quad + \frac{101}{2}e^4 \cos(2t) + \frac{107}{4}e^3 \cos(3t) + \frac{197}{4}e^4 \cos(4t) + O(e^5) \\
 N_5(e, t) &= 1 + \frac{27}{2}e^2 + \frac{573}{8}e^4 + 8e \cos t + 65e^3 \cos t + 22e^2 \cos 2t \\
 &\quad + \frac{400}{3}e^4 \cos(2t) + 51e^3 \cos(3t) + \frac{1283}{12}e^4 \cos(4t) + O(e^5). \quad (\text{A.9})
 \end{aligned}$$

This expansion is valid for small values of the eccentricity (for example those considered in Table A.1); larger values of the eccentricity would need a series development to a higher degree. As we did for the model (6) we compute the BAM associated to the model (1)–(A.8)–(A.9) over a random set of 1,000 initial data, for $\varepsilon = 10^{-3}$, $K = 10^{-4}$ and various values of eccentricity. The results reported in Table A.1 show that the models (1)–(A.8)–(A.9) and (6) provide very similar behaviors, indicating that the oscillations of the terms $\frac{a^6}{r^6}$ and $\frac{a^6}{r^6} \dot{f}$ can be neglected in a first approximation. The numbers reported in Table A.1 for the time-dependent and the averaged model are typically of the same order of magnitude.

References

Arnold, V.I. (eds.): Encyclopedia of Mathematical Sciences. Dynamical Systems III, vol. 3. Springer-Verlag (1988)

Biasco, L., Chierchia, L.: On the basins of attraction of low-order resonances in weakly dissipative spin-orbit models (2008) (Preprint)

Broer, H.W., Huitema, G.B., Sevryuk, M.B.: Quasi-periodic Motions in Families of Dynamical Systems. Order Amidst Chaos. Lecture Notes in Mathematics, 1645. Springer-Verlag, Berlin (1996)

Broer, H.W., Simó, C., Tatjer, J.C.: Towards global models near homoclinic tangencies of dissipative diffeomorphisms. *Nonlinearity* **11**, 667–770 (1998)

Celletti, A.: Analysis of resonances in the spin-orbit problem in Celestial Mechanics: The synchronous resonance (Part I). *J. Appl. Math. Phys. (ZAMP)* **41**, 174–204 (1990)

Celletti A., Chierchia L.: KAM tori for N-body problems (a brief history), *Celest. Mech. Dyn. Astr.* **95**, 117–139 (2006)

Celletti, A., Chierchia, L.: Quasi-periodic attractors in celestial mechanics. *Arch. Ration. Mech. Anal.* (2008). <http://www.mat.uniroma3.it/users/chierchia/PREPRINTS/QPA.pdf> (to appear)

Colombo, G., Shapiro, I.I.: The rotation of the planet Mercury. *Astrophys. J.* **145**, 296–307 (1966)

Correia, A.C.M., Laskar, J.: Mercury’s capture into the 3/2 spin-orbit resonance as a result of its chaotic dynamics. *Nature* **429**, 848–850 (2004)

Cox, A.N. (ed.): *Allen’s Astrophysical Quantities*. Springer, New York (2000)

- Feudel, U., Grebogi, C., Hunt, B.R., Yorke, J.A.: A map with more than 100 coexisting low-period periodic attractors. *Phys. Rev. E* **54**, 71–81 (1996)
- Goldreich, P., Peale, S.J.: Spin-orbit coupling in the Solar System. *Astron. J.* **71**(6), 425–438 (1966)
- Goldreich, P., Peale, S.J.: The dynamics of planetary rotations. *Ann. Rev. Astron. Astrophys.* **6**, 287–320 (1970)
- Henrard, J.: Spin-orbit resonance and the adiabatic invariant. In: Ferraz-Mello S., Sessin W. (eds.) *Resonances in the Motion of Planets, Satellites and Asteroids*, pp. 19–26, IAG-USP, São Paulo (1985)
- Laskar, J.: Large scale chaos and marginal stability in the Solar System. *Celest. Mech. Dyn. Astr.* **64**, 115–162 (1996)
- MacDonald, G.J.F.: Tidal friction. *Rev. Geophys.* **2**, 467–541 (1964)
- Peale, S.J.: The free precession and libration of Mercury. *Icarus* **178**, 4–18 (2005)
- Wisdom, J., Peale, S.J., Mignard, F.: The chaotic rotation of Hyperion. *Icarus* **58**, 137–152 (1984)
- Yoshida, H.: Construction of higher order symplectic integrators. *Phys. Lett. A* **150**, 262–268 (1990)